COMMUNICATION

Solution-Grown Organic Single-Crystalline p-n Junctions with Ambipolar Charge Transport

Congcheng Fan, Arjan P. Zoombelt, Hao Jiang, Weifei Fu, Jiake Wu, Wentao Yuan, Yong Wang, Hanying Li, Hongzheng Chen,* and Zhenan Bao*

Single-crystals of organic semiconductors have the potential to show the best charge transport properties among organic materials. High-performance single-crystal electronic devices typically consist of one type of single crystal, favoring either hole or electron transport. Devices composed of both hole and electron transporting single-crystals, such as single-crystalline p-n junctions, are expected to exhibit ambipolar charge transport that is desirable for complementary circuits,[1] organic light emitting diodes (OLEDs),[2] and organic solar cells.[3] However, it is challenging to prepare organic single-crystalline p-n junctions on which there are only a few reports.[4] Here, we describe the growth of single-crystalline p-n junctions in a single step from a mixed solution of 2,7-dioctyl[1]benzothieno[3,2-b][1]benzothiophene (C8-BTBT) (p-type) and C_{60} (n-type), using the droplet-pinned crystallization (DPC) method previously reported.[5] These junctions exhibited ambipolar charge transport characteristics in field-effect transistors (FETs) with the best performance of 0.16 $cm^2\ V^{-1}\ s^{-1}$ for hole mobility and 0.17 $cm^2\ V^{-1}\ s^{-1}$ for electron mobility, respectively. This work provides a new platform to study organic single-crystalline p-n junctions.

Single crystals of organic semiconductors, with the highest degree of order and purity, have been shown to exhibit high electronic performance such as the superior charge carrier mobility among organic materials.[6–8] The techniques for fabrication of FETs based on organic single crystals have been progressing quickly toward high mobility.[9–11] Currently, both hole and electron mobility of these devices have reached above 10 $cm^2\ V^{-1}\ s^{-1}$.[5,12–18] In addition to FETs, organic single crystals can be used for other optoelectronic devices, such as solar cells,[19] light-emitting transistors,[20,21] OLEDs,[22] and optical complexer[23] and might be further used for electrical driven organic laser.[24] Typically, high-performance single-crystal electronic devices are fabricated from one type of organic material where either hole or electron transport dominates. Intuitively, devices composed of both hole and electron transporting single crystals, such as single-crystalline p-n junctions, can enable additional electronic properties including ambipolar transport and exciton generation/dissociation at the junctions. Although FETs based on two components (p- and n-channels) have been prepared to achieve ambipolar transport[25–30] and mixtures of donor and acceptor were widely used for organic solar cells,[31,32] the crystallinity of the semiconducting materials is usually low and the device performance is moderate. In order to further improve the crystallinity for both fundamental studies and high-performance electronic applications, organic single-crystalline p-n junctions are desired. However, single-crystalline p-n junctions are difficult to prepare since crystallization generally requires relatively clean environments and crystallization of two components together tends to interrupt each other. Recently, highly crystalline heterostructures of rubrene and a α-quaterthiophene were prepared by organic molecular beam epitaxy (OMBE).[33] Furthermore, copper hexadecafluorophthalocyanine (n-type) crystals were grown onto copper phthalocyanine (p-type) crystals to form single-crystalline p-n junctions using physical vapor transport (PVT).[4] Both OMBE and PVT methods require high temperature and atmosphere control (ultra-high vacuum or inert gas) and low yield is to be expected. In comparison, crystallization from solution is a more convenient method. However, solution-grown organic single-crystalline p-n junctions have not been achieved. Previously, single-crystal-based two-phase heterostructures were prepared through solution methods where one phase formed around the other phase preformed.[23,34,35] In context of these results, we envision that crystallization from a solution of a mixture of p- and n-type materials should be possible to result in single-crystalline p-n junctions if one crystal (e.g., n-type crystal) grows first and, subsequently, the other (e.g., p-type crystal) nucleates on the former. In this work, we demonstrated this approach by preparing crystals from a mixed solution of C8-BTBT and C_{60}. We obtained single-crystalline p-n junctions and investigated their ambipolar transport characteristics.

C8-BTBT and C_{60} were used to grow single-crystalline p-n junctions. C_{60} is a typical electron transporting material with mobilities as high as 11 $cm^2\ V^{-1}\ s^{-1}$,[5,36–38] while C8-BTBT is among the best hole transporting organic materials.[14,39–41] Before growing crystals from their mixed solution, we examined crystallization from solutions with only one component (either C8-BTBT or C_{60}). For both C8-BTBT and C_{60}

C. C. Fan, H. Jiang, W. F. Fu, J. K. Wu,
Prof. H. Y. Li, Prof. H. Z. Chen
State Key Laboratory of Silicon Materials
MOE Key Laboratory of Macromolecular Synthesis and Functionalization
Department of Polymer Science and Engineering
Zhejiang University
Hangzhou, 310027, P. R. China
E-mail: hanying_li@zju.edu.cn; hzchen@zju.edu.cn
W. T. Yuan, Prof. Y. Wang
State Key Laboratory of Silicon Materials
Center of Electron Microscopy
Department of Materials Science and Engineering
Zhejiang University
Hangzhou, 310027, P. R. China
A. P. Zoombelt, Prof. Z. N. Bao
Department of Chemical Engineering
Stanford University
Stanford, California, 94305, USA

DOI: 10.1002/adma.201302605

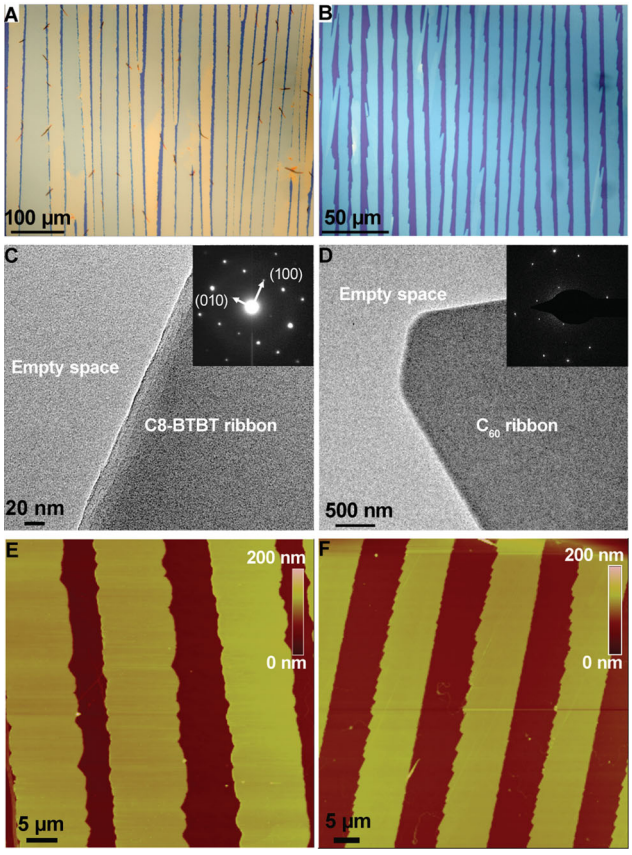

Figure 1. The morphology and crystalline structures of C8-BTBT and C_{60} ribbons grown by the DPC method. (A,B) Optical microscopy (OM) images of well-aligned (A) C8-BTBT and (B) C_{60} ribbons. (C,D) TEM images and SAED patterns (insets) of (C) C8-BTBT ribbon and (D) C_{60} ribbon. (E,F) AFM images of (E) C8-BTBT ribbons and (F) C_{60} ribbons.

solutions, aligned ribbon crystals were grown using the DPC method.[5,42,43] (**Figure 1**A,B,E,F) Similar to other aligned crystallization directed by concentration and/or temperature gradients,[44–47] crystals were aligned during the directional droplet receding driven by surface tension (**Figure 2**A). The thickness of the ribbon crystals depends on the concentration of the semiconductor solutions. For the typical concentration (0.4 mg mL^{-1}) we used, it is about 60 nm measured by atomic force microscope (AFM). Transmission electron microscopy (TEM) and selected area electron diffraction (SAED) indicated that both C8-BTBT and C_{60} form single-crystalline ribbons by showing single sets of diffraction spots (Figure 1C,D).[5,39] The C8-BTBT ribbons exhibit the same color and brightness when rotated under cross polarizers, as a supporting evidence for the single-crystallinity (Figure S1, Supporting Information).

In order to obtain p-n junctions of C8-BTBT and C_{60}, a solution of a mixture of C8-BTBT and C_{60} in m-xylene and carbon tetrachloride was used in the DPC process. Similar to the crystallization from solutions with one component (Figure 1A,B), we also obtained aligned ribbon-like crystals from the mixed solutions (Figure 2B,C). Interestingly, two types of ribbons overlapped each other, with the light-yellow ribbons always on top of the blue ones. The AFM height profile clearly shows one piece of ribbon is on top of the other (Figure 2D). According to the color, the light-yellow ribbons were assigned as C8-BTBT and the blue ones as C_{60}, which was further confirmed by Raman mapping and SAED. Raman intensity map using the 1355–1509 cm^{-1} region (characteristic Raman shift of C_{60}, Figure S3) in an area where three blue ribbons were partly covered by light-yellow ribbons indicated that the blue regions were C_{60} while the light yellow crystals on top were not (Figure 2C). TEM revealed that the ribbons partly overlapped and SAED at the non-overlapping regions showed a single set of diffraction pattern consistent with the previously-reported C8-BTBT single crystals and C_{60} ribbon-like single crystals grown from the same solvents (Figure 2E-G).[5,39] Therefore, the OM, Raman, AFM, TEM and SAED evidences demonstrate that we obtained the single-crystalline p-n junctions of C8-BTBT ribbon and C_{60} ribbon.

The growth of single-crystalline organic p-n junctions directly from a mixture of both p- and n-type semiconductors has not been reported before. We speculate that two important requirements should be satisfied to grow the crystalline p-n junctions from a mixed solution. First, two crystalline organic semiconductors should have different growth rate. One molecule crystallizes easier and grows first. Subsequently, the other nucleates on the former heterogeneously (Figure 2A). These sequential crystallization events were recorded in Movie S1 where the C_{60} crystals grew faster as the growth fronts of the blue C_{60} ribbons were closer to the receding contact line than those of the light-yellow C8-BTBT ribbons. As a result, the two phases (C8-BTBT and C_{60}) separated, with the slow-growing C8-BTBT light-yellow ribbons always existing on the top layer of the double-layer regions (Figure 2B,C). Second, the pinner of the DPC method provides a steady growth condition by avoiding the sliding of the solution droplets (Figure 2A). Without the pinner, crystals grow randomly and even discontinuously (Figure S2A,B).

After obtaining the single-crystalline p-n junctions of C8-BTBT and C_{60}, we proceeded to examine their charge transport properties. Bottom-gate and top-contact FETs (channel length 50 μm, width 1 mm) were fabricated and the ambipolar characteristics were investigated. The typical transfer characteristics of the devices are shown in **Figure 3**A and B, exhibiting classic V-shaped curves, wherein the two arms stand for electron transport and hole transport, respectively. The output characteristics in p-channel (Figure 3C) and n-channel (Figure 3D) operation modes confirmed the excellent gate modulation. The best FET performance was achieved from the C8-BTBT and C_{60} single-crystalline p-n junction grown from a solution ([C8-BTBT] = 0.6 mg mL^{-1}, [C_{60}] = 0.2 mg mL^{-1}), with the most balanced hole and electron mobility of 0.16 cm^2 V^{-1} s^{-1} and 0.17 cm^2 V^{-1} s^{-1}, respectively. The histograms of hole and electron mobility obtained from 50 devices based on p-n junctions are shown in Figure 3E,F. For hole transport, hole mobility (μ_h) ranging from 0.012 to 0.29 cm^2 V^{-1} s^{-1}, on-to-off current ratios (I_{on}/I_{off}) > 10 and threshold voltages (V_T) between −63.5 to −75.7 V were achieved. For electron transport, we obtained electron mobility (μ_e) ranging from 0.0031 to 0.21 cm^2 V^{-1} s^{-1}, I_{on}/I_{off} > 10, and V_T between 20.2 to 72.1 V. The mobility values are underestimated because neither C8-BTBT nor C_{60} ribbons completely cover the whole channel of the devices. For comparison, we also examined the unipolar characteristics of 50 C8-BTBT based p-channel transistors and 50 C_{60} based

ADVANCED MATERIALS
www.advmat.de

www.MaterialsViews.com

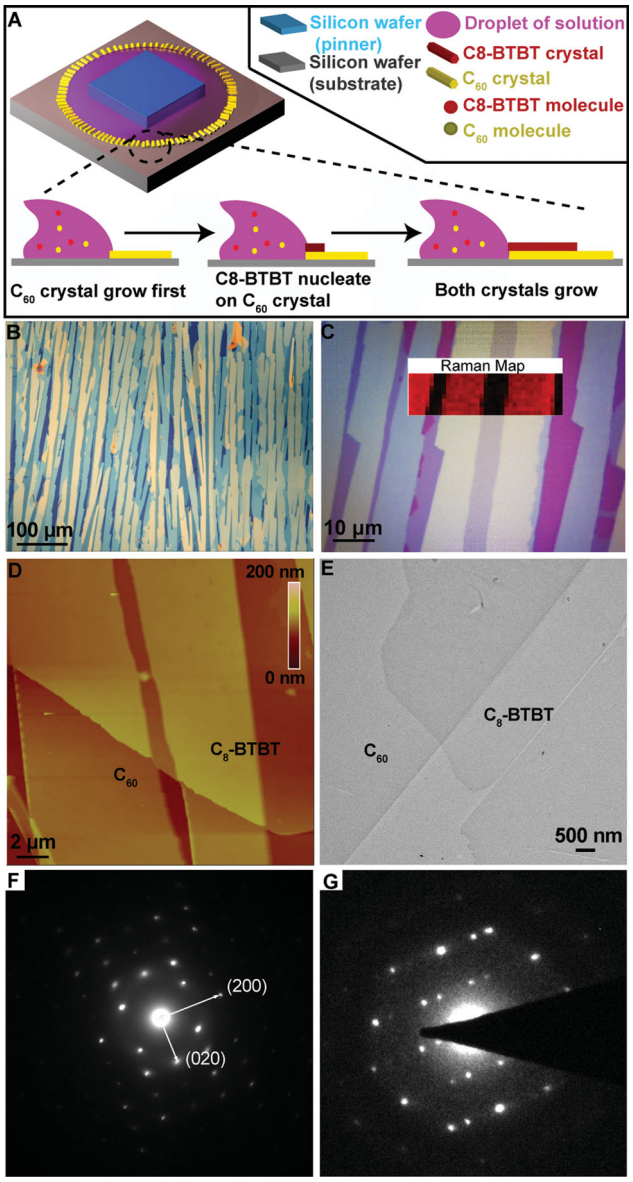

Figure 2. Schematic presentations of the DPC method and the morphology and crystalline structures of C8-BTBT ribbon and C_{60} ribbon single-crystalline p-n junctions grown from a solution ([C8-BTBT] = 0.2 mg mL^{-1}, [C_{60}] = 0.2 mg mL^{-1}). (A) The typical DPC method to grow well-aligned single crystals. For growth of p-n junctions, a mixed solution of C8-BTBT and C_{60} is used. C_{60} crystallizes first and C8-BTBT nucleates on it heterogeneously. Subsequently, both crystals grow simultaneously into junctions. (B,C) OM images of C8-BTBT ribbon and C_{60} ribbon p-n junctions. The blue ribbons are C_{60} crystals, while the light yellow ones are C8-BTBT crystals; Inset in C: A Raman intensity map of the 1355–1509 cm^{-1} region (Raman shift of C_{60}, Figure S3) in an area where three blue ribbons were partly covered by light-yellow ribbons. (D) An AFM image of the p-n junction, showing C8-BTBT ribbon on top of C_{60} ribbon. (E) A TEM image showing C8-BTBT and C_{60} ribbons stacking together. (F,G) SAED patterns of individual C8-BTBT ribbon and C_{60} ribbon respectively, indicating the single-crystallinity.

n-channel devices, respectively. For C8-BTBT ribbons, μ_h ranging from 0.055 to 0.60 $cm^2\ V^{-1}\ s^{-1}$, $I_{on}/I_{off} > 10^4$ and V_T between −54.5 to −75.8 V were achieved. These mobility values are a little below the reported ones.[14,39–41] Also, the value is underestimated due to the incomplete channel coverage. For C_{60} ribbons, μ_e ranging from 0.0055 to 0.087 $cm^2\ V^{-1}\ s^{-1}$, $I_{on}/I_{off} > 10^3$ and V_T between 41.3 to 77.7 V were obtained. The devices were measured in air and the mobility value is lower than the previous one measured in glovebox.[5] Compared to the hole and electron mobility of the single semiconductor, the mobility values of the p-n junctions are comparable but slightly lower. In addition to the different channel coverage, the disparity may be due to the slight incorporation of one molecule inside the crystal of the other and therefore potential crystal lattice disruption.

Besides ribbon-like p-n junctions, we also changed the solvent to m-xylene in order to vary the shape of the C_{60} crystals. As a result, we obtained C8-BTBT ribbon and C_{60} needle p-n junctions.[5] OM images clearly showed that ribbon crystals overgrew from the needle crystals to form junctions (**Figure 4**A,B). AFM and TEM images confirmed the contacting between the two crystals in the junctions (Figure 4C,D). The SAED of an individual ribbon exhibited spot patterns indicative of C8-BTBT single crystals (Figure 4E),[39] while a high-resolution TEM (HRTEM) study of the needle showed a two-dimensional (2-D) lattice image consistent with the previously-reported hexagonal structure of C_{60}•m-xylene crystals grown from the same solvent (Figure 4F).[5,48] Therefore, the OM, AFM and TEM evidences allowed us to conclude that we obtained single-crystalline junctions from C8-BTBT ribbons and C_{60} needles. FETs based on these junctions also exhibited ambipolar charge transport characteristics. As the crystals were grown from a mixed solution ([C8-BTBT] = 2.0 mg mL^{-1}, [C_{60}] = 1.0 mg mL^{-1}), the FET devices showed the best performance of 0.16 ± 0.06 $cm^2\ V^{-1}\ s^{-1}$ for hole mobility and $6.1 \pm 3.8 \times 10^{-5}$ $cm^2\ V^{-1}\ s^{-1}$ for electron mobility, respectively. The low mobility values of C_{60} needles are mostly due to low channel coverage and air instability.

In summary, we demonstrated a simple yet efficient method to prepare organic single-crystalline p-n junctions from solutions of a mixture of organic semiconductors. Both C8-BTBT ribbon/C_{60} ribbon and C8-BTBT ribbon/C_{60} needle single-crystalline p-n junctions have been prepared by selecting proper solvents and evaporation processes. FETs based on the junctions showed ambipolar charge transport characteristics, with the best performance of 0.16 $cm^2\ V^{-1}\ s^{-1}$ for hole mobility and 0.17 $cm^2\ V^{-1}\ s^{-1}$ for electron mobility, respectively that are among the highest reported mobilities of single-crystal-based ambipolar organic transistors.[49,50] Compared to the ambipolar devices composed of separated organic single crystals,[42,50–54] the contacting p-n single crystals reported here promise ideal interfaces at the junctions for exciton generation/dissociation. As such, these single-crystalline p-n junctions provide a platform to deepen the fundamental knowledge and to fabricate high-performance electronic devices of organic semiconductors.

Experimental Section

C8-BTBT was synthesized according to the literature procedure[55,56] and subsequently purified by multiple recrystallizations from hexane. Crystals were grown in-situ on the substrates for FETs using the DPC method.[5] The substrates were BCB-covered highly doped silicon substrates (1 cm^2) with 300 nm SiO_2. BCB (Dow Chemicals) thin-layers were

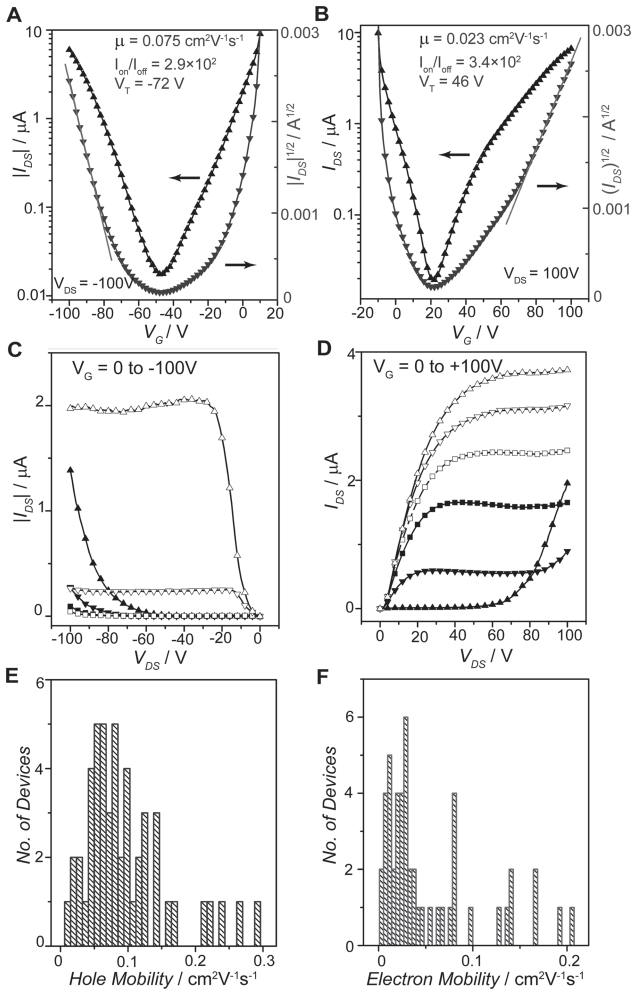

Figure 3. FET Characteristics of C8-BTBT ribbon and C_{60} ribbon single-crystalline p-n junctions. (A,C) Typical transfer (A) and output (C) characteristics in p-channel operation mode under negative drain bias. (B,D) Typical transfer (B) and output (D) characteristics in n-channel operation mode under positive drain bias. (E,F) Histogram of hole (E) and electron (F) mobility calculated from 50 devices based on the single-crystalline p-n junctions.

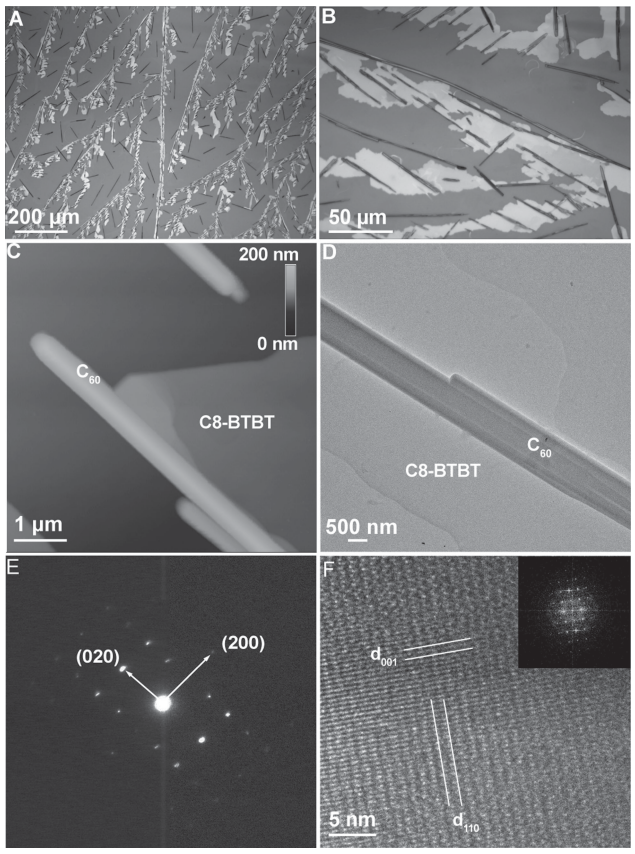

Figure 4. Morphology and crystalline structures of C8-BTBT ribbon and C_{60} needle single-crystalline p-n junctions grown from a solution ([C8-BTBT] = 0.2 mg mL^{-1}, [C_{60}] = 0.2 mg mL^{-1}). (A, B) OM images of C8-BTBT ribbon and C_{60} needle p-n junctions. (C) An AFM image of the p-n junction, showing a C8-BTBT ribbon overgrown from a C_{60} needle. (D) A TEM image of the junction, showing C8-BTBT ribbon and C_{60} needle grown together. (E) SAED patterns of C8-BTBT ribbon, indicating its single-crystallinity. (F) A HRTEM image of C_{60} needle, showing 2-D lattice of C_{60}·m-xylene single crystal; (inset) fast Fourier transform (FFT) of (F).

spin-coated from a mesitylene (Fluka) solution (volume ratio of BCB to mesitylene, 1:30) and then thermally cross-linked on a hotplate in a N_2 glovebox. C8-BTBT and C_{60} solution (20 μL) was dropped on a silicon substrate (1 cm^2) with a smaller piece of silicon wafer (0.4 × 0.4 cm^2, pinner) to pin the solution droplet. The silicon substrate was placed on a Teflon slide inside a Petri-dish (35 × 10 mm) sealed with parafilm, allowing the solvent to slowly evaporate on a hotplate of 25 ± 1 °C. The solution dried out within 2 h and aligned C8-BTBT and C_{60} crystals formed together. For the growth of C8-BTBT ribbons and C_{60} needles, m-xylene (Sigma-Aldrich) was used as a solvent and the concentration ranged from 0.2 to 2.0 mg mL^{-1} for C8-BTBT and 0.2 to 1.0 mg mL^{-1} for C_{60}. For the growth of C8-BTBT ribbons and C_{60} ribbons, mixed solvents of m-xylene and carbon tetrachloride (CCl_4, Aladdin; volume ratio of m-xylene to CCl_4, 1:1) were used and the concentration ranged from 0.2 to 0.8 mg mL^{-1} for C8-BTBT and 0.2 to 0.4 mg mL^{-1} for C_{60}. As control experiments, single-component ribbon crystals (either C8-BTBT or C_{60}, [C8-BTBT] = 0.4 mg mL^{-1}, [C_{60}] = 0.2 mg mL^{-1}) were also grown using the DPC method. The morphology of the crystals were characterized by OM (Nikon LV100 POL), Raman microscopy (Renishaw InVia Raman Microscope), and AFM (Veeco 3D). The crystalline structures were examined by TEM (FEI Tecnai F20, 200 kV). FETs were constructed in bottom-gate, top-contact configuration by depositing source and drain electrodes (70 nm Au), with channel length (L) of 50 μm and width (W) of 1 mm. The ambipolar properties of transistors were measured in air with an Agilent 4155C parameter analyzer. The measured capacitance of the BCB-covered SiO_2/Si substrates was 10 nF cm^{-2}, and this value was used for mobility calculation.

Supporting Information

Supporting Information is available from the Wiley Online Library or from the author.

Acknowledgements

This work was supported by the National Natural Science Foundation of China (Grants: 51222302, 50990063, 91233114), Zhejiang Province

Natural Science Foundation (Grant: LZ13E030002), the Scientific Research Foundation for the Returned Overseas Chinese Scholars, State Education Ministry, and Fundamental Research Funds for the Central Universities (2012QNA4025).

Received: June 7, 2013
Published online: August 16, 2013

[1] B. Crone, A. Dodabalapur, Y.-Y. Lin, R. W. Filas, Z. Bao, A. LaDuca, R. Sarpeshkar, H. E. Katz, W. Li, *Nature* **2000**, *403*, 521–523.
[2] C. W. Tang, S. A. VanSlyke, *Appl. Phys. Lett.* **1987**, *51*, 913.
[3] C. W. Tang, *Appl. Phys. Lett.* **1986**, *48*, 183.
[4] Y. J. Zhang, H. L. Dong, Q. X. Tang, S. Ferdous, F. Liu, S. C. B. Mannsfeld, W. P. Hu, A. L. Briseno, *J. Am. Chem. Soc.* **2010**, *132*, 11580–11584.
[5] H. Y. Li, B. C. K. Tee, J. J. Cha, Y. Cui, J. W. Chung, S. Y. Lee, Z. N. Bao, *J. Am. Chem. Soc.* **2012**, *134*, 2760–2765.
[6] V. Podzorov, *Mrs Bull.* **2013**, *38*, 15–24.
[7] R. J. Li, W. P. Hu, Y. Q. Liu, D. B. Zhu, *Acc. Chem. Res.* **2010**, *43*, 529–540.
[8] C. Reese, Z. N. Bao, *Mater. Today* **2007**, *10*, 20–27.
[9] V. Podzorov, V. M. Pudalov, M. E. Gershenson, *Appl. Phys. Lett.* **2003**, *82*, 1739.
[10] H. Y. Li, G. Giri, J. B.-H. Tok, Z. N. Bao, *Mrs Bull.* **2013**, *38*, 34–42.
[11] J. G. Mei, Y. Diao, A. L. Appleton, L. Fang, Z. N. Bao, *J. Am. Chem. Soc.* **2013**, *135*, 6724–6746.
[12] V. Podzorov, E. Menard, A. Borissov, V. Kiryukhin, J. A. Rogers, M. E. Gershenson, *Phys. Rev. Lett.* **2004**, *93*, 086602.
[13] V. C. Sundar, J. Zaumseil, V. Podzorov, E. Menard, R. L. Willett, T. Someya, M. E. Gershenson, J. A. Rogers, *Science* **2004**, *303*, 1644–1646.
[14] H. Minemawari, T. Yamada, H. Matsui, J. Tsutsumi, S. Haas, R. Chiba, R. Kumai, T. Hasegawa, *Nature* **2011**, *475*, 364–367.
[15] O. D. Jurchescu, M. Popinciuc, B. J. van Wees, T. T. M. Palstra, *Adv. Mater.* **2007**, *19*, 688–692.
[16] J. Takeya, M. Yamagishi, Y. Tominari, R. Hirahara, Y. Nakazawa, T. Nishikawa, T. Kawase, T. Shimoda, S. Ogawa, *Appl. Phys. Lett.* **2007**, *90*, 102120.
[17] J. H. Oh, H. W. Lee, S. Mannsfeld, R. M. Stoltenberg, E. Jung, Y. W. Jin, J. M. Kim, J.-B. Yoo, Z. N. Bao, *Proc. Natl. Acad. Sci. U. S. A.* **2009**, *106*, 6065–6070.
[18] A. S. Molinari, H. Alves, Z. Chen, A. Facchetti, A. F. Morpurgo, *J. Am. Chem. Soc.* **2009**, *131*, 2462–2463.
[19] R. J. Tseng, R. Chan, V. C. Tung, Y. Yang, *Adv. Mater.* **2008**, *20*, 435–438.
[20] H. Nakanotani, M. Saito, H. Nakamura, C. Adachi, *Adv. Funct. Mater.* **2010**, *20*, 1610–1615.
[21] S. Z. Bisri, T. Takenobu, Y. Yomogida, H. Shimotani, T. Yamao, S. Hotta, Y. Iwasa, *Adv. Funct. Mater.* **2009**, *19*, 1728–1735.
[22] M. Pope, H. P. Kallmann, P. Magnante, *J. Chem. Phys.* **1963**, *38*, 2042–2043.
[23] Y. J. Li, Y. L. Yan, C. Zhang, Y. S. Zhao, J. N. Yao, *Adv. Mater.* **2013**, *25*, 2784–2788.
[24] H. Wang, F. Li, I. Ravia, B. Gao, Y. P. Li, V. Medvedev, H. Sun, N. Tessler, Y. G. Ma, *Adv. Funct. Mater.* **2011**, *21*, 3770–3777.
[25] S. J. Noever, S. Fischer, B. Nickel, *Adv. Mater.* **2013**, *25*, 2147–2151.
[26] M. Cavallini, P. D'Angelo, V. V. Criado, D. Gentili, A. Shehu, F. Leonardi, S. Milita, F. Liscio, F. Biscarini, *Adv. Mater.* **2011**, *23*, 5091–5097.
[27] S. R. Puniredd, A. Kiersnowski, G. Battagliarin, W. Zajączkowski, W. W. H. Wong, N. Kirby, K. Müllen, W. Pisula, *J. Mater. Chem. C* **2013**, *1*, 2433–2440.
[28] Q. S. Wei, K. Tajima, K. Hashimoto, *Acs Appl. Mater. Interfaces* **2009**, *1*, 1865–1868.
[29] J. Wang, H. B. Wang, X. J. Yan, H. C. Huang, D. Jin, J. W. Shi, Y. H. Tang, D. H. Yan, *Adv. Funct. Mater.* **2006**, *16*, 824–830.
[30] E. J. Meijer, D. M. de Leeuw, S. Setayesh, E. van Veenendaal, B.-H. Huisman, P. W. M. Blom, J. C. Hummelen, U. Scherf, T. M. Klapwijk, *Nat. Mater.* **2003**, *2*, 678–682.
[31] G. Yu, J. Gao, J. C. Hummelen, F. Wudl, A. J. Heeger, *Science* **1995**, *270*, 1789–1791.
[32] Y. Z. Lin, Y. F. Li, X. W. Zhan, *Chem. Soc. Rev.* **2012**, *41*, 4245–4272.
[33] A. Sassella, L. Raimondo, M. Campione, A. Borghesi, *Adv. Mater.* **2013**, *25*, 2804–2808.
[34] H. Y. Li, H. L. Xin, D. A. Muller, L. A. Estroff, *Science* **2009**, *326*, 1244–1247.
[35] M. Sindoro, Y. H. Feng, S. X. Xing, H. Li, J. Xu, H. L. Hu, C. C. Liu, Y. W. Wang, H. Zhang, Z. X. Shen, H. Y. Chen, *Angew. Chem. Int. Ed.* **2011**, *50*, 9898–9902.
[36] T. D. Anthopoulos, B. Singh, N. Marjanovic, N. S. Sariciftci, A. Montaigne Ramil, H. Sitter, M. Cölle, D. M. de Leeuw, *Appl. Phys. Lett.* **2006**, *89*, 213504.
[37] X. H. Zhang, B. Kippelen, *J. Appl. Phys.* **2008**, *104*, 104504.
[38] C.-Z. Li, C.-C. Chueh, H.-L. Yip, J. Zou, W.-C. Chen, A. K.-Y. Jen, *J. Mater. Chem.* **2012**, *22*, 14976.
[39] P. S. Jo, A. Vailionis, Y. M. Park, A. Salleo, *Adv. Mater.* **2012**, *24*, 3269–3274.
[40] T. Minari, C. Liu, M. Kano, K. Tsukagoshi, *Adv. Mater.* **2012**, *24*, 299–306.
[41] Y. Z. Chen, B. Lee, H. T. Yi, S. S. Lee, M. Payne, S. Pola, C.-H. Kuo, L. Loo, J. E. Anthony, Y.-T. Tao, *Phys. Chem. Chem. Phys.* **2012**, *14*, 14142–14151.
[42] H. Y. Li, B. C. K. Tee, G. Giri, J. W. Chung, S. Y. Lee, Z. N. Bao, *Adv. Mater.* **2012**, *24*, 2588–2591.
[43] H. Y. Li, J. G. Mei, A. L. Ayzner, M. F. Toney, J. B.-H. Tok, Z. N. Bao, *Org. Electron.* **2012**, *13*, 2450–2460.
[44] W. Pisula, A. Menon, M. Stepputat, I. Lieberwirth, U. Kolb, A. Tracz, H. Sirringhaus, T. Pakula, K. Müllen, *Adv. Mater.* **2005**, *17*, 684–689.
[45] L. Q. Li, P. Gao, K. C. Schuermann, S. Ostendorp, W. C. Wang, C. Du, Y. Lei, H. Fuchs, L. D. Cola, K. Müllen, L. F. Chi, *J. Am. Chem. Soc.* **2010**, *132*, 8807–8809.
[46] G. Schweicher, N. Paquay, C. Amato, R. Resel, M. Koini, S. Talvy, V. Lemaur, J. Cornil, Y. Geerts, G. Gbabode, *Cryst. Growth Des.* **2011**, *11*, 3663–3672.
[47] G. Giri, E. Verploegen, S. C. B. Mannsfeld, S. Atahan-Evrenk, D. H. Kim, S. Y. Lee, H. A. Becerril, A. Aspuru-Guzik, M. F. Toney, Z. N. Bao, *Nature* **2011**, *480*, 504–508.
[48] C. Park, H. J. Song, H. C. Choi, *Chem. Commun.* **2009**, 4803.
[49] J. Zhang, J. H. Tan, Z. Y. Ma, W. Xu, G. Y. Zhao, H. Geng, C. A. Di, W. P. Hu, Z. G. Shuai, K. Singh, D. B. Zhu, *J. Am. Chem. Soc.* **2013**, *135*, 558–561.
[50] T. Uemura, M. Yamagishi, Y. Okada, K. Nakayama, M. Yoshizumi, M. Uno, J. Takeya, *Adv. Mater.* **2010**, *22*, 3938–3941.
[51] A. L. Briseno, R. J. Tseng, S.-H. Li, C.-W. Chu, Y. Yang, E. H. L. Falcao, F. Wudl, M.-M. Ling, H. Z. Chen, Z. N. Bao, H. Meng, C. Kloc, *Appl. Phys. Lett.* **2006**, *89*, 222111.
[52] Q. X. Tang, Y. H. Tong, W. P. Hu, Q. Wan, T. Bjørnholm, *Adv. Mater.* **2009**, *21*, 4234–4237.
[53] J. Soeda, T. Uemura, Y. Mizuno, A. Nakao, Y. Nakazawa, A. Facchetti, J. Takeya, *Adv. Mater.* **2011**, *23*, 3681–3685.
[54] A. L. Briseno, S. C. B. Mannsfeld, C. Reese, J. M. Hancock, Y. J. Xiong, S. A. Jenekhe, Z. N. Bao, Y. N. Xia, *Nano Lett.* **2007**, *7*, 2847–2853.
[55] M. Saito, T. Yamamoto, I. Osaka, E. Miyazaki, K. Takimiya, H. Kuwabara, M. Ikeda, *Tetrahedron Lett.* **2010**, *51*, 5277–5280.
[56] H. Ebata, T. Izawa, E. Miyazaki, K. Takimiya, M. Ikeda, H. Kuwabara, T. Yui, *J. Am. Chem. Soc.* **2007**, *129*, 15732–15733.